Theoretical Study of the Internal Rotation of the Hydroxylic Group of the Enol Form of Guanine

Jean Cadet, André Grand, and Christophe Morell

Département de Recherche Fondamentale sur la Matière Condensée, Service de Chimie Inorganique et Biologique, Laboratoire des Lesions des Acides Nucleiques, (UMR=5046), CEA-Grenoble, France

Jorge R. Letelier

Departamento de Quımica, FCFM, Universidad de Chile, Casilla 2777, Santiago, Chile

José Luis Moncada and Alejandro Toro-Labbé*

QTC, Facultad de Química, Pontificia Universidad Católica de Chile, Casilla 306, Correo 22, Santiago, Chile

Received: August 29, 2002; In Final Form: February 20, 2003

Emphasis was placed in the present work on a density functional theory and Hartree−Fock study of the internal rotation of the hydroxylic group of the enol form of guanine. This was achieved by monitoring the behavior of energy, chemical potential, hardness, electrophilicity, and polarizability along the torsional coordinate. An energy barrier of about 9.5 kcal/mol was found about midway between two stable planar conformations. The analysis of the behavior of reactivity descriptors shows that the principles of maximum hardness and minimum polarizability are satisfied. Very good linear relations have been established between energy, chemical potential, hardness, and electrophilicity power allowing the characterization of the rotational process in terms of the simultaneous change of these global properties.

1. Introduction

In this paper, emphasis was placed on the study of the internal rotation process of the hydroxylic group of the enol form of guanine (see Figure 1). We study the evolution, along the torsional angle θ, of the potential energy V, electronic chemical potential μ, molecular hardness η, electrophilicity index ω, and polarizability α. Our main goal is to characterize the internal rotation process in terms of the simultaneous evolution of the energy and various electronic global properties and look for consistency among them. In particular, we are interested in characterizing the transition state and the potential barrier involved in the rotational process.

Guanine is a nucleobase that together with other pyrimidine and purine components are responsible of the structure of DNA and RNA. Because damage to DNA may occur through chemical changes induced to its purine and pyrimidine bases, by radiation,[1] electron transfer,[2] or the action of different kinds of chemical species that may produce in changes of the molecular conformation, it is interesting to characterize low energy activation processes such as the internal rotation in the isolated tautomers to check how difficult it might be to produce those conformational changes through the action of the above-mentioned external perturbations. Global and local electronic properties are response functions to different kinds of perturbations; therefore, a study of the internal rotation needs a complete characterization of the torsional potential energy and electronic properties.

Three tautomeric forms of guanine are presented in Figure 1. **G1**, the keto form, is very close in energy to **G2**, the enol form; they are in tautomeric equilibrium.[3] **G2** is in turn in conformational equilibrium with **G3**. In this paper, we are going to study the isomerization reaction **G2** → **G3** that takes place through internal rotation of the hydroxylic group, as shown in Figure 1.

Density functional theory (DFT)[4−6] has provided the conceptual basis to define powerful tools aimed at characterizing chemical structures and their global and local reactivity properties. Within the frame of DFT, a complete characterization of an N-particle wave function needs only N and the external potential $v(b > r)$, so the energy of the system may be expressed as a function of the electron number N and a functional of the external potential $v(\vec{r})$: $E[\rho(\vec{r})] \equiv E[N, v(\vec{r})]$. The total differential of the energy is given by[4]

$$dE = \mu\, dN + \int \rho(\vec{r})\, dv(\vec{r})\, d\vec{r} \qquad (1)$$

where

$$\mu = \left(\frac{\partial E}{\partial N}\right)_v$$

and

$$\rho(\vec{r}) = \left[\frac{\delta E}{\delta v(\vec{r})}\right]_N \qquad (2)$$

are the chemical potential and the ground-state electron density, respectively. The chemical potential is a global property that characterizes the escaping tendency of electrons from the equilibrium system;[7] formally, it is the Lagrange multiplier associate with the normalization constraint of DFT that the

* To whom correspondence should be addressed. E-mail: atola@puc.cl.

10.1021/jp021976w CCC: $25.00
Published on Web 06/17/2003

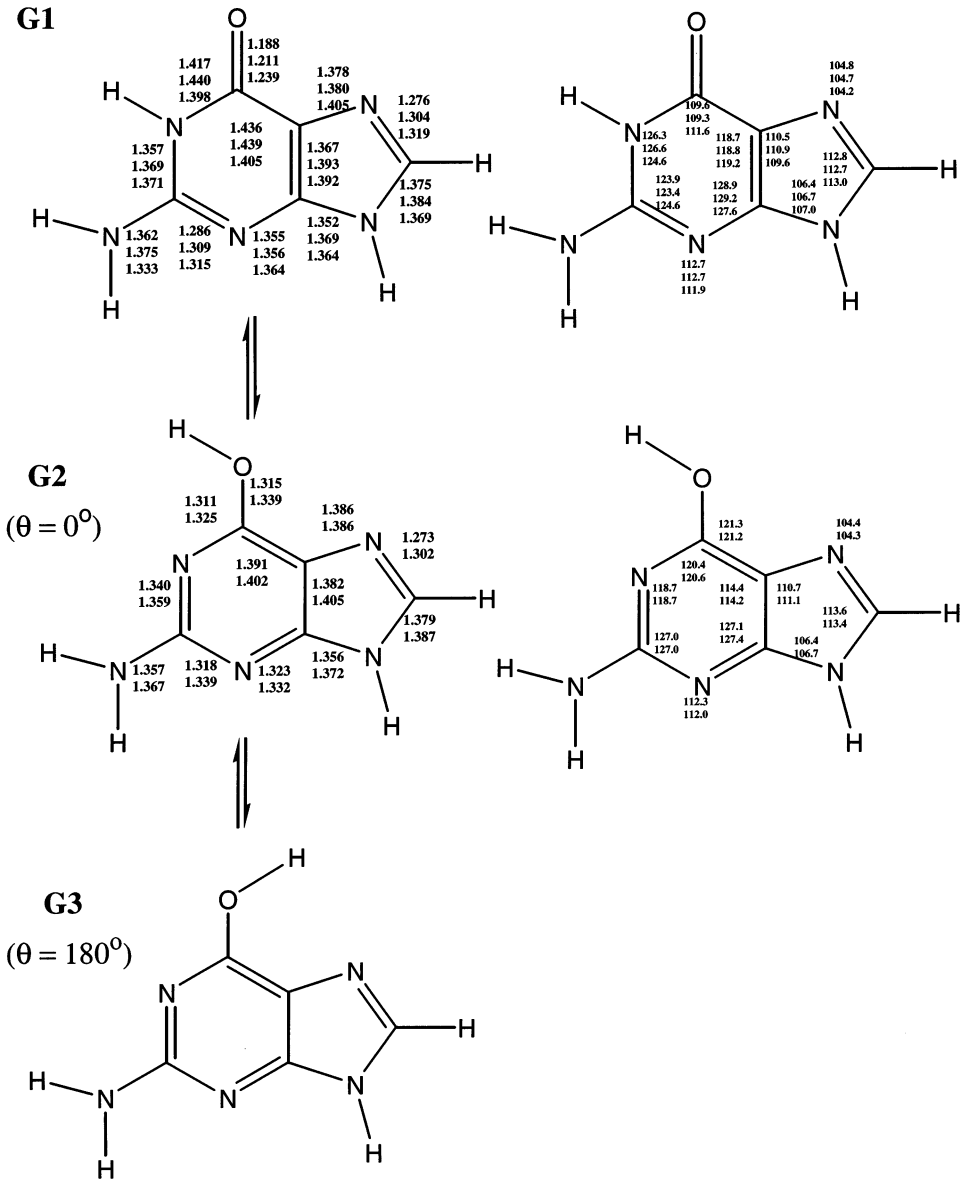

Figure 1. Calculated and experimental structural parameters of the systems considered in this paper. The values on the molecules are ordered as follows: upper, HF/6-311G**; middle, DFT/B3LYP/6-311G**; lower, experimental.

electron density integrates to N, the total number of electrons.[4] μ is in turn a function of N and a functional of $v(b > r)$, so that $\mu \equiv \mu[N, v(b > r)]$, and therefore its total differential is

$$d\mu = \eta\, dN + \int f(\vec{r})\, dv(\vec{r})\, d\vec{r} \qquad (3)$$

where

$$\eta = \frac{1}{2}\left(\frac{\partial \mu}{\partial N}\right)_v$$

and

$$f(\vec{r}) = \left[\frac{\delta \mu}{\delta v(\vec{r})}\right]_N = \left(\frac{\partial \rho(\vec{r})}{\partial N}\right)_v \qquad (4)$$

are the hardness[8−11] and the Fukui function[12,13] of the system, respectively. η can be seen as a resistance to charge transfer; it is a global property of the system and depends on both N and $v(\vec{r})$. μ and η are global properties that are related to well-established chemistry concepts through the electronegativity (χ) that has been found to be the negative of the chemical potential ($\mu = -\chi$).[4,8] Chemical potential and hardness are responses of the system when N is varied for a fixed external potential $v(\vec{r})$, complementary to μ and η, and the polarizability (α) may be used in understanding the behavior of the system for changing $v(\vec{r})$ at constant N.

The use of the above reactivity properties is better characterized within the context of a few principles and equations widely used in classical reactivity theory to characterize chemical reactions and transition states. The Hammond postulate (HP) [14] interrelates the position of the transition state (TS) to the exothermicity of the reaction, and it states that the TS is similar in structure to the energy-nearest adjacent stable complex. The Leffler's postulate[15] defines the position of the TS through the Brønsted coefficient, β, a similarity index that can be interpreted as the degree of resemblance of the TS with respect to the product.[16] The Marcus equation (ME),[17] originally proposed to characterize electron-transfer reactions, provides a simple expression for the activation energy that is consistent with both, the Hammond's and Leffler's postulates. Connection between DFT concepts and classical chemistry principles is achieved

through the principle of maximum hardness (PMH).[18,19] The PMH asserts that molecular systems at equilibrium tend to states of high hardness, and as a consequence, TS's are expected to present a minimum value of hardness.[20,21] Along with this, Chattaraj et al have proposed the minimum polarizability principle (MPP) which states that the natural direction of evolution of any system is toward a state of minimum polarizability.[22,23] In the context of chemical reactivity, the PMH and MPP complement the minimum energy criterion for molecular stability, and this in turn helps characterize transition states. In this paper, we shall use the above-mentioned principles of reactivity in chemistry to rationalize the profiles of energy and electronic properties along the torsional angle.

The paper is organized as follows: after this introduction, section 2 presents the theoretical backgrounds; computational details and calculation methodologies employed in this work are described in section 3; section 4 is devoted to the discussion of the results; and Section 5 contains our concluding remarks.

2. Theoretical Background

Torsional Potential Energy and Transition State. The reaction coordinate is the torsional angle θ defined with respect to the CO bond and taking as reference the dihedral angle NCOH: $\theta \equiv \angle$(NCOH) (see Figure 1: **G2**,**G3**). We express the torsional potential through the following function that comes out from a truncated Fourier expansion:[24]

$$V(\theta) = \frac{1}{4}\mathrm{K_V}(1 - \cos^2\theta) + \frac{1}{2}\Delta V^\circ(1 - \cos\theta) \qquad (5)$$

where $\mathrm{K_V} = k_t + k_c$ and $\{k_t, k_c\}$ are the forces constants associated with the N-cis ($\theta = 0°$) and N-trans ($\theta = 180°$) potential wells; $\Delta V^\circ = [V(180°) - V(0°)]$ is the reaction energy, where the origin of the energy has been chosen at $\theta = 0°$, thus $V(0°) = 0$. From the above equation, the position of the transition state at $\theta = \theta°$ can be determined through

$$\left(\frac{\mathrm{d}V}{\mathrm{d}\theta}\right)_{\theta=\theta^\circ} = 0 \Rightarrow \cos\theta^\circ = -\frac{\Delta V^\circ}{K_\mathrm{V}} \qquad (6)$$

Introducing the above result into eq 5, we obtain an expression for the energy of the transition state (TS)[24,25]

$$\Delta V^{\ddagger}_{\mathrm{m}} = \frac{1}{4}K_\mathrm{V} + \frac{1}{2}\Delta V^\circ + \frac{(\Delta V^\circ)^2}{4K_\mathrm{V}} \qquad (7)$$

which is equivalent to the Marcus equation.[17] The position of the TS can be rationalized through the use of the Brønsted coefficient that, following the Leffler postulate,[15] is defined as the derivative of the activation energy with respect to the reaction energy. Use of the Marcus expression, eq 7, leads to

$$\beta \equiv \left(\frac{\mathrm{d}\Delta V^{\ddagger}_{\mathrm{m}}}{\mathrm{d}\Delta V^\circ}\right) = \frac{1}{2} + \frac{\Delta V^\circ}{2K_\mathrm{V}} \qquad (8)$$

Consistency of eq 7 with the calculated barrier height can be checked through direct comparison of $\Delta V^{\ddagger}_{\mathrm{m}}$ with $\Delta V^{\ddagger}_{\mathrm{opt}}$, the potential barrier determined through full optimization of the TS structure. Similarly, the Brønsted coefficient should be compared with the value determined at the optimized TS structure, using eq 6 to obtain

$$\beta_{\mathrm{opt}} = \frac{1}{2}(1 - \cos\theta_\circ) \qquad (9)$$

Chemical Potential, Hardness, Electrophilicity, and Polarizability. In most numerical applications, chemical potential and molecular hardness are calculated using the finite difference approximation that leads to μ and η in terms of the ionization potential (I) and electron affinity (A).[4−6] Further approximations, involving the use of the Koopmans theorem, give access to μ and η in terms of the energies of frontier molecular orbitals HOMO and LUMO. The following approximate versions of μ and η have been widely used:[4−6]

$$\mu \approx \frac{1}{2}(I + A) = \frac{1}{2}(\epsilon_\mathrm{L} + \epsilon_\mathrm{H}) \qquad (10)$$

and

$$\eta \approx \frac{1}{2}(I - A) = \frac{1}{2}(\epsilon_\mathrm{L} - \epsilon_\mathrm{H}) \qquad (11)$$

where ϵ_H and ϵ_L are the energies of the HOMO and LUMO molecular orbitals, respectively.

Another important reactivity descriptor is the electrophilicity index ω. It measures the energy stabilization upon electronic saturation of the system when electrons flow from the surroundings with a higher chemical potential than that of the system. The electrophilicity index is defined in terms of μ and η as[26,27]

$$\omega = \frac{\mu^2}{2\eta} = \frac{\mu^2}{2}S \qquad (12)$$

where $S = 1/\eta$ is the softness of the system, another global property of the system.[4]

The set of descriptors μ, η, and ω are the response of the system when changing N at constant external potential. However, in all chemical processes, the external potential change so we also need to know the response of the system when $v(r)$ is varied for a fixed N. This can be measured indirectly through the polarizability α, that accounts for the electronic reorganization induced by an external field. The mean polarizability $\langle\alpha\rangle$ is a descriptor that can be used to understand the behavior of the system for changing $v(r)$ at constant N. $\langle\alpha\rangle$ is calculated as the arithmetic average of the diagonal component of the polarizability tensor[28,29]

$$\langle\alpha\rangle = \frac{1}{3}(\alpha_{xx} + \alpha_{yy} + \alpha_{zz}) \qquad (13)$$

The polarizability has been related to the softness;[30] thus, a highly polarizable system is expected to be more reactive or softer than a less polarizable system that is expected to be hard and stable.[22,23,29]

3. Computational Details

The profiles of global properties were obtained through SCF ab initio calculations at the Hartree−Fock (HF) and DFT levels with the standard 6-311G** basis set using the package Gaussian 98.[31] For the DFT calculations, the B3 (Becke 3) functional was used together with the Lee, Yang, and Parr functional (LYP) for describing correlation and exchange.[32,33] The torsional potential energy and electronic properties were evaluated every 10 ° increments along θ within the interval $0° \le \theta \le 180°$. To characterize the effect of electronic correlation, MP2 calculations[34] were performed at the critical points with the HF optimized structures. On the other hand, chemical potential, hardness, and electrophilicity were calculated using the HOMO and LUMO frontier orbitals, through eqs 10 and 11. Validating

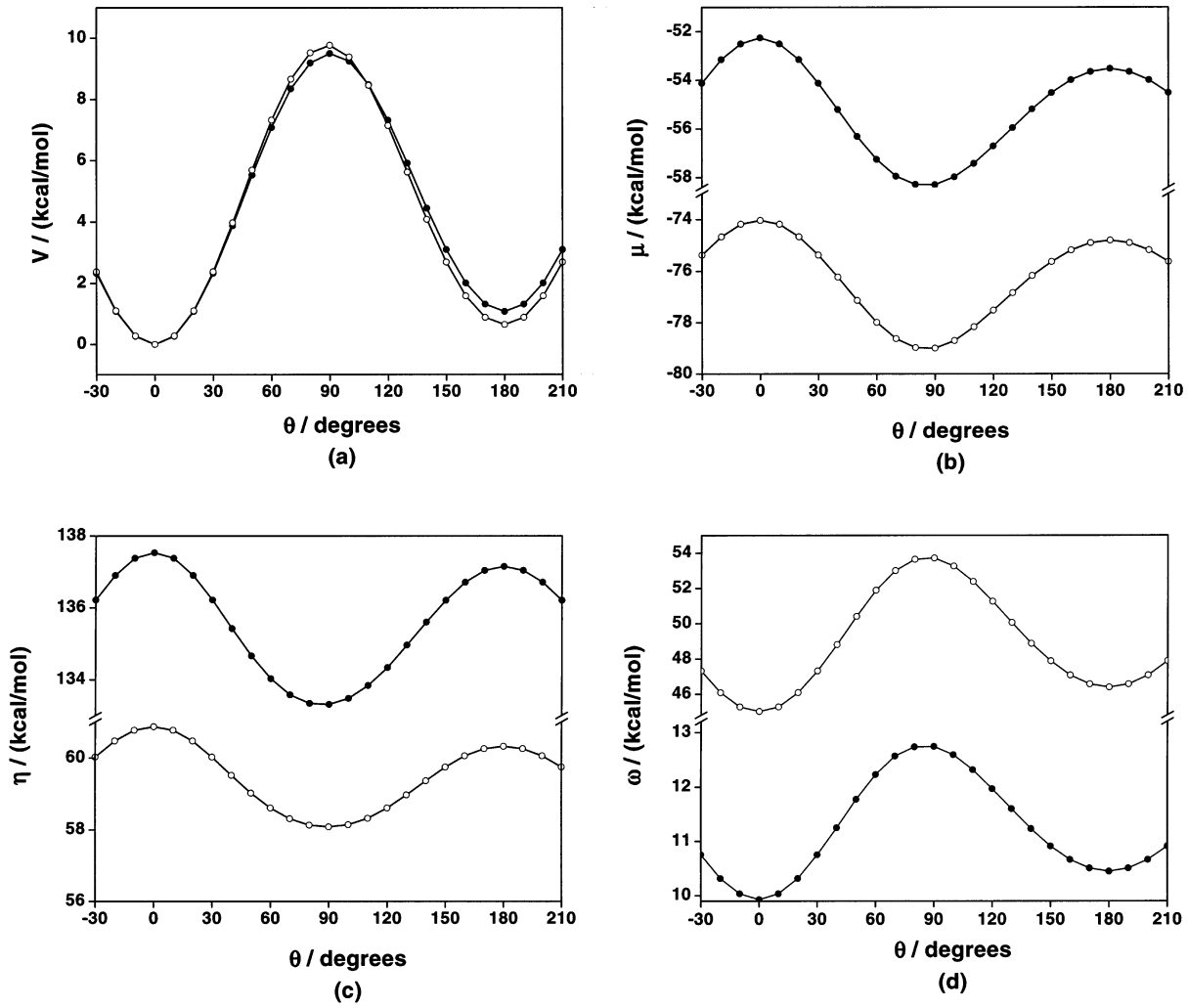

Figure 2. HF/6-311G** (black circles) and DFT/B3LYP/6-311G** (open circles) profiles of energy (a), chemical potential (b), hardness (c), and electrophilicity (d) along the torsional angle θ.

the use of the Koopmans theorem in the calculation of μ and η is the negative value of the HF/6-311G** HOMO energy that compares very well with the experimental ionization potential: the calculated value is 8.23 eV, and the experimental value is 8.24 eV.[35,36] In contrast to this, the negative of the B3LYP/6-311G** HOMO energy is only 5.85 eV, much lower than the experimental value. In the frame of the DFT Kohn−Sham theory, the Koopmans theorem normally underestimate the first ionization potential,[37] and moreover, it is only applicable for the exact density functional for which it has been shown that the negative of the ionization potential is equal to the HOMO energy.

The polarizability tensor components were determined analytically as the second derivative of the energy with respect to the Cartesian components of the electric field.

4. Results and Discussion

4.1. Molecular Structure, Energy, and Electronic Properties. *Molecular Structure.* The geometric parameters of isomers **G2** and **G3** were optimized at the HF and B3LYP levels. The resulting molecular parameters are given in Figure 1, and the available experimental data are also included.[38] Note that, because there is no experimental information about the structure of the enol form of guanine, the calculated geometry of the purine ring was compared with the X-ray structure of **G1**. It is interesting to note that our results on the molecular structure are in quite good agreement with the X-ray data with quite small errors of about 2% in both HF and DFT calculations.

In Figure 2 are displayed the HF and DFT profiles of torsional potential energy (a), chemical potential (b), hardness (c), and electrophilicity (d). The behavior of these properties upon internal rotation is discussed in the following paragraphs, and at first sight shows that the torsional dependence of V, μ, η, and ω is quite well represented by both calculations (HF and DFT) obtaining in all cases the same overall trends.

Energy Profile. HF and DFT energy profiles are displayed in Figure 2a. It may be noted that both profiles are very close to each other and present a maximum at about midway between the cis and trans conformations; the barriers are 9.50 kcal/mol at the HF level and 9.73 kcal/mol using B3LYP. The most stable conformation is found at $\alpha = 0°$, a conformation that seems to be favored by the attractive local interaction among the hydrogen of the enol group and the neighboring nitrogen electron pair of the adjacent imidazole ring. In Table 1 are quoted the numerical values of parameters quantifying the isomerization reaction, and these are the reaction energy ($\Delta V°$), the optimized and Marcus potential barriers ($\Delta V^{\ddagger}_{opt}$ and $\Delta V^{\ddagger}_{m}$), and the Brønsted coefficients (β_{opt} and β). To determine $\Delta V^{\ddagger}_{m}$, eq 7 is used with the values of $\Delta V°$ given in Table 1, and the parameter $K_V = (k_t + k_c)$ was determined from the k_t and k_c values that in turn were obtained through fitting the individual cis and trans potential energy wells to localized harmonic potentials functions.[24]

TABLE 1: Torsional Potential Energy Parameters Determined at Different Levels of Calculation for the Internal Rotation of Hydroxy-Guanine[a]

parameters	HF	B3LYP	MP2
$\Delta V°$	1.07	0.64	0.59
K_V	35.74	37.62	27.99
$\Delta V^{\ddagger}_{m}$	9.48	9.73	7.29
$\Delta V^{\ddagger}_{opt}$	9.50	9.77	9.24
β	0.51	0.51	0.49
β_{opt}	0.50	0.49	0.50

[a] Energies are given in kcal/mol.

The energy barriers predicted using the Marcus expression (HF and B3LYP) displayed in Table 1 are in very good agreement with the corresponding optimized values; however, at the MP2 level, these values differs by about 2 kcal/mol, a departure that may be attributed to an inaccurate estimation of the force constants needed to define the parameter K_V. Indeed, when using the eq 7 to determine K_V from $\Delta V^{\ddagger}_{opt}$ and $\Delta V°$, the MP2 data produces $K_V = 35.8$ kcal/mol, which is very close to the HF and B3LYP results. On the other hand, comparison of the HF and MP2 optimized energies shows that the effect of electronic correlation on the potential barrier is small although it is crucial for estimating the reaction energy, and this result is confirmed by the B3LYP data. In all cases, the parameter giving the position of the TS (β) is very close to the reference optimized value, and all these results indicate that the scheme to analyze the torsional isomerization reaction **G2** $\rightleftharpoons$ **G3** based on the Marcus equation is adequate for this system.

Chemical Potential. Changes in chemical potential result from electron density reordering occurring in any dynamical process, this produces charge transfer from systems with high values of μ to systems with low values of μ until the chemical potential reaches an equilibrium value. This picture to rationalize variations of chemical potential is applied to internal rotations where the isomers connected through the torsional angle present different values of their electronic and structural properties. Figure 2b shows that the chemical potential, both HF and DFT, exhibits a behavior with considerable variations along the torsional angle, and μ presents maxima at the reference conformations and a minimum at the TS. Changes in chemical potential indicate that rearrangements of the electronic density are taking place, and a variation of μ during the internal rotation can be explained in terms of electron transfer from conformations with high values of μ to conformations with low values of μ. In the present case, the electronic flux goes from the reference stable conformations toward the TS. Moreover, the amount of flowing charge is proportional to the difference in the chemical potential of the molecule at different conformations,[7] and an estimation of the intramolecular charge transfer (ΔN) when going from θ_1 to θ_2 can be obtained through the following expression:[4,7]

$$\Delta N = \frac{1}{2}\frac{[\mu(\theta_2) - \mu(\theta_1)]}{[\eta(\theta_2) + \eta(\theta_1)]} \qquad (14)$$

that, at the HF level, leads to $\Delta N \sim -0.01$ (-0.02 at the B3LYP level) when going from the cis conformation ($\theta = 0$) to the transition state ($\theta = \theta°$) and $\Delta N \sim +0.009$ ($+0.018$ at the B3LYP level) when going from the TS to the trans isomer. The rearrangement of the electron density is confirmed by the fact that the dipole moment, at the HF level, changes from about 3.0 D at the cis conformation to 3.4 D at the TS to reach a value of about 3.8 D at the trans conformation.

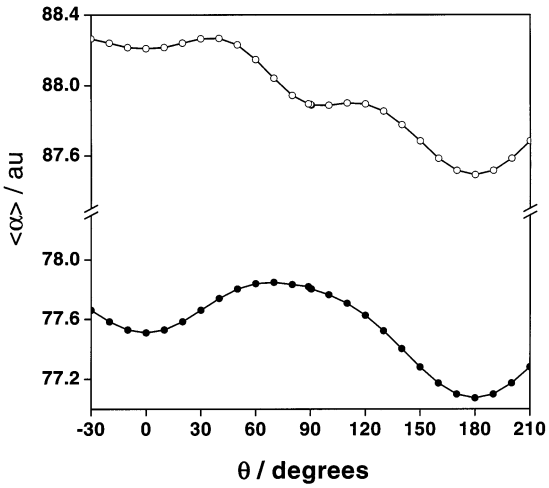

Figure 3. HF/6-311G** (black circles) and DFT/B3LYP/6-311G** (open circles) profiles of polarizability along the torsional angle θ.

Molecular Hardness. Figure 2, parts a and c, shows that V and η, both HF and DFT, present opposite behavior along the torsional angle thus satisfying the PMH,[18,19] and stable conformations are harder than the TS, which present a minimum of η. Indeed, it can be appreciated that the cis conformation is slightly harder than the trans conformation, in agreement with what should be expected from the PMH and the relative stability of the isomers.

It should be noted that, although a minimum at the TS for the hardness profile may also be expected on other grounds than the PMH,[39] consistency of the results in terms of their expected qualitative behavior around the TS substantiate the use of the frontier orbitals HOMO and LUMO to determine μ and η and the PMH as a qualitative tool to characterize the behavior of hardness at the TS. Although the chemical potentials do not remain constant along the reaction coordinate, the PMH holds; however, the behavior of μ in connection with the PMH is still unclear. Indeed, it has been recently pointed out that there are cases where constancy of μ is not a sufficient condition for the PMH to hold.[40]

Electrophilicity. The conformational dependence of the electrophilicity index is displayed in Figure 2d where we note that the TS is highly electrophilic, whereas the stable conformations present minimum values of ω. It is interesting to note that μ and ω behave in opposite ways along θ, and because electrons flow from a conformation with high chemical potential to a conformation with low chemical potential, a minimum μ is expected for a conformation having a relatively high electrophilic power whereas a conformation presenting a maximum value of μ must be less electrophilic because it should be saturated of electrons.

Polarizability. In Figure 3 are displayed the HF and DFT profiles of polarizability, it should be noticed that the HF profile complies with the minimum polarizability principle exhibiting minima at the stable conformations and a maximum at the TS. In contrast to this, the DFT calculation presents a peculiar behavior that verifies the MPP at the stable conformations, but it is against the MPPs expectations at the TS. This behavior of the B3LYP polarizability does not prevent us from having overall good values for this property. The B3LYP polarizability of the cis conformation, $\bar{\alpha}(0°) = 88.21$ au, is in very good agreement with the experimental polarizability, $\bar{\alpha}(0°) = 91,8$ au.[41]

4.2. Rationalization of the Isomerization Reaction. *The* $\{\mu, \eta, V\}$ *Representation.* Because the HF and DFT profiles of all

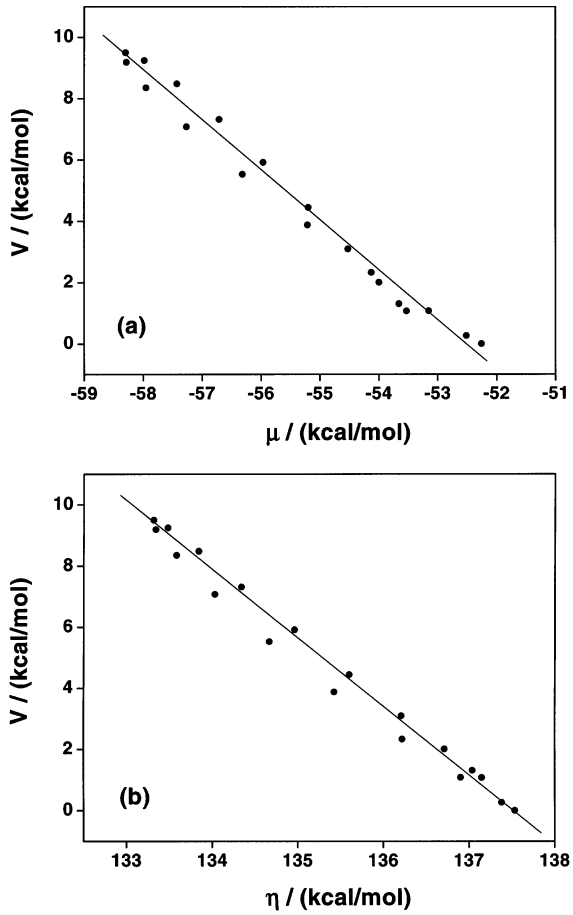

Figure 4. HF/6-311G** correlations of the energy profile with the chemical potential (a) and hardness (b) profiles.

properties analyzed so far are qualitatively alike, only the HF results will be used to rationalize the internal rotation process. From the observed qualitative behavior of V, μ, and η along the torsional angle, it can be concluded that all of these properties are correlated. Figure 4 shows good linear correlations among the energy and the electronic properties μ and η. This result show that the internal rotation of the enol form of guanine is a reaction case in which the isomerization process can be characterized in the frame of the $\{\mu, \eta, V\}$ representation.[25,42]

In recent papers,[25,42] it has been shown that when the profiles of V, μ, and η are interrelated they can be studied simultaneously by expressing the potential energy as a functional of both the chemical potential and hardness, $V(\theta) \equiv V[\mu(\theta),\eta(\theta)]$, as they were independent variables. This is an approximation that is valid only in cases where the energy is strongly correlated with the electronic properties, as observed in Figure 4. The total differential of such a functional is therefore

$$dV = \left(\frac{\partial V}{\partial \mu}\right)_\eta d\mu + \left(\frac{\partial V}{\partial \eta}\right)_\mu d\eta = Q_\eta\, d\mu + Q_\mu\, d\eta \qquad (15)$$

where we have defined the coefficients $Q_\eta = (\partial V/\partial \mu)_\eta$ and $Q_\mu = (\partial V/\partial \eta)_\mu$. Under the above depicted approximation, eq 15 indicates that all energy variations are determined by changes in μ and η only, the response of the system when N is varied. This indicates that the effect of changes in the external potential is less important in the characterization of the torsional potential energy.

For a finite variation of the potential energy, we can write

$$\Delta V = Q_\eta \Delta\mu + Q_\mu \Delta\eta \qquad (16)$$

which is valid for all θ. Because μ and η are independently correlated with the energy (Figure 4), their slopes should give reasonably good approximations to the parameters Q_η and Q_μ even though in this approximation they are not calculated at constant hardness and chemical potential, respectively. The numerical values of these coefficients are given by the half of the slopes of Figure 4, parts a and b: $Q_\eta = -0.817$ and $Q_\mu = -1.097$; the factor $^1/_2$ on these slopes were introduced to take care for the correct combination of the μ and η dependence of the torsional potential V.[25] In this context, the torsional potential as a functional of μ and η is therefore defined through the above slopes, and this approximation is valid as long as the coefficients Q_η and Q_μ remain reasonably constant along the reaction coordinate allowing the linear correlations displayed in Figure 4. This is a necessary condition for expressing the energy in terms of μ and η, as independent variables in eqs 15 and 16. If this is so, the $\{Q_\eta, Q_\mu\}$ parameters can be related to the amount of charge redistributed during the chemical process,[25] and the physical meaning of Q_η and Q_μ is going to be apparent later on when discussing the connection between torsional potential and electrophilicity.

Because eq 16 is valid for all θ, in particular, it allows an expression for the energy of the transition state in terms of the activation chemical potential and hardness[25,42]

$$\Delta V^\ddagger = Q_\eta \Delta\mu^\ddagger + Q_\mu \Delta\eta^\ddagger \qquad (17)$$

Using the numerical values of the coefficients $\{Q_\eta, Q_\mu\}$ together with the calculated activation chemical potential and hardness ($\Delta\mu^\ddagger = -6.01$ kcal/mol; $\Delta\eta^\ddagger = -4.22$ kcal/mol), the torsional potential barrier is estimated to be 9.54 kcal/mol, in perfect agreement with the optimized value displayed in Table 1 ($\Delta V^\ddagger = 9.50$ kcal/mol). This result shows that consistency between energy and the electronic global properties μ and η was achieved thus grounding the approximations used in rationalizing the results.

Relation between Torsional Potential and Electrophilicity Profiles. Figure 2, parts a and d, shows that V and ω feature the same overall trend suggesting that they might be correlated. This observation prompts us to compare $V[\mu,\eta]$ with the variation along θ of the electrophilicity index which is also a functional of both μ and η, as can be noticed in eq 12. The total differential of ω is

$$d\omega = \left(\frac{\mu}{\eta}\right) d\mu - \frac{1}{2}\left(\frac{\mu}{\eta}\right)^2 d\eta \qquad (18)$$

and for finite variations it can be written

$$\Delta\omega = -\left(\Delta N_{max}\cdot\Delta\mu + \frac{1}{2}\Delta N_{max}{}^2\cdot\Delta\eta\right) \qquad (19)$$

where $\Delta N_{max} = -\mu/\eta$, defined as the maximum electronic charge that the electrophile may accept,[26,43] has been used. Note that eqs 18 and 19 are similar to eqs 15 and 16 and valid for all θ. Formally, ΔN_{max} depends on the torsional angle, but it can be verified in Figure 5, which shows the profile of ΔN_{max} along θ, which it changes slightly in the range of 0.38 and 0.44. ΔN_{max} presents a maximum value at the TS, a result that is consistent with the minimum of the chemical potential and the maximum electrophilicity power at that point.

The electrophilicity at the TS can be estimated from eq 19, thus obtaining

$$\Delta\omega^\ddagger = -\left(\Delta N_{max}\cdot\Delta\mu^\ddagger + \frac{1}{2}\Delta N_{max}{}^2\cdot\Delta\eta^\ddagger\right) \qquad (20)$$

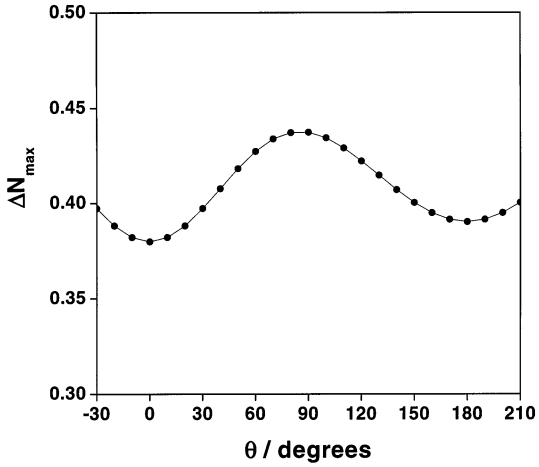

Figure 5. Profile of the maximum charge transferred during the internal rotation of the enol group.

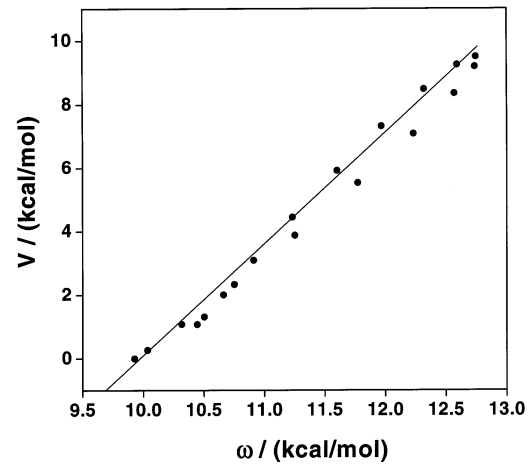

Figure 6. HF/6-311G** correlation of the torsional potential energy and electrophilicity profiles along the torsional angle θ.

use of the average value of ΔN_{max} (0.41) together with the already reported values for the activation chemical potential and hardness leads to $\Delta\omega^{\ddagger} = 2.82$ kcal/mol in perfect agreement with the actual calculated value.

Figure 6 confirms the expected correlation among V and ω (correlation factor $r = 0.99$) for this system. Within this context, the torsional potential energy can then be written in terms of the electrophilicity index along the torsional angle as $V(\theta) = a + b\, w(\theta)$, the boundary conditions at $\theta = 0$, $V(0) = 0$, lead to $a = -b\, w(0)$; at $\theta = \theta°$, $V(\theta°) = \Delta V^{\ddagger}$, leads to $b = \Delta V^{\ddagger}/\Delta\omega^{\ddagger}$; the condition $V(180) = \Delta V°$ leads to redundant data. A linear fit of the points displayed in Figure 6 leads to the following numerical values for these parameters $a = -34.79$ kcal/mol and $b = 3.47$, which are in quite good agreement with what is obtained from their analytic definitions ($a = -33.46$ kcal/mol and $b = 3.37$).

Consistency between energy and electronic properties may now be analytically achieved by putting $\Delta V^{\ddagger} = b\cdot\Delta\omega^{\ddagger}$ and using eqs 17 and 20, thus leading to

$$Q_\eta \Delta\mu^{\ddagger} + Q_\mu \Delta\eta^{\ddagger} = -b\left(\Delta N_{max}\cdot\Delta\mu^{\ddagger} + \frac{1}{2}\Delta N_{max}{}^2\cdot\Delta\eta^{\ddagger}\right) \quad (21)$$

this confirms the relation of the parameters $\{Q_\eta, Q_\mu\}$ with the amount of charge available for transfer during the chemical process[25]

$$Q_\eta = -b\,\Delta N_{max}; \qquad Q_\mu = -\frac{1}{2} b\,\Delta N_{max}{}^2 \quad (22)$$

The above equations relating parameters coming out from independent data fittings procedures might be used to check consistency between V, μ, η, and ω. Use of $b = 3.37$ together with the average value of ΔN_{max} leads to $Q_\eta = -1.38$ and $Q_\mu = -0.28$, values that, although different from the original values determined from Figure 4, parts a and b, produces the correct value for the barrier height (9.47 kcal/mol) and a quite acceptable value for the reaction energy of $\Delta V° = 1.83$ kcal/mol, lying within acceptable limits of $\pm$ 1 kcal/mol around the corresponding reference value. On the other hand, if the original from fitting values of $Q_\eta = -0.82$ and $Q_\mu = -1.10$ are used, then values of 0.24 and 0.57 for ΔN_{max} are obtained from Q_η and Q_μ [eq 2], respectively; the average of them is 0.41, which is exactly the mean value of ΔN_{max} along θ. Either way, the above results show quite good consistency and are defining upper and lower limits for the parameters involved.

Corollary of the Energy-Electrophilicity Relation. Because total softness is a sum of local contributions centered on the different atoms in the molecule ($S = \sum s_k$),[4-6] global electrophilicity, eq 12, can be written in terms of local contributions as

$$\omega = \frac{\mu^2}{2\eta} = \frac{1}{2}\mu^2\cdot S = \frac{1}{2}\mu^2 \sum_k s_k = \sum_k \omega_k \quad (23)$$

with $\omega_k = \mu^2 s_k/2$ being the local electrophilicity power associated to center k. Use of eq 23 together with $V(\theta) = a + b\,\omega(\theta)$ leads to an empiric partition of the potential energy in terms of n local contributions

$$V(\theta) = \sum_k^n V_k(\theta) = \sum_k^n \left(\frac{a}{n} + b\,\omega_k(\theta)\right) \quad (24)$$

Partition of the energy from the above considerations allows one to identify specific centers that might be responsible for a given behavior of the energy at a given point along the torsional angle. In particular, this may throw light into the characterization of the nature of potential barriers in internal rotation processes.

5. Concluding Remarks

In this work, a DFT and HF study of the internal rotation of the hydroxylic group of the enol form of guanine has been presented. This was achieved by monitoring the behavior of energy, chemical potential, hardness, electrophilicity, and polarizability along the torsional coordinate. The analysis of the behavior of reactivity descriptors shows that the principles of maximum hardness and minimum polarizability are satisfied and consistency between different electronic properties and energy was achieved within acceptable error limits.

Very good linear relations have been established between energy, chemical potential, and hardness allowing the characterization of the rotational process in terms of the simultaneous change of these global properties.

The transition state for the internal rotation process has been characterized through its position along the torsional angle and its potential energy barrier. This later has been rationalized in terms of the activation chemical potential, hardness, and electrophilicity power.

Provided a good correlation between energy and electrophilicity, an empiric energy partition has been proposed, in particular, it may help characterize the nature of potential

barriers by determining the contribution of specific atomic centers and identifying their interactions.

External perturbations may produce noticeable conformational changes on the tautomers of guanine, and this is accompanied with energy transfer toward or from the reference system. The overall conformational and energetic change of the system can be understood in terms of the changes induced on few electronic global properties. The results discussed in this paper show that the internal rotation of the hydroxylic group of the enol form of guanine can be correctly rationalized through the use of DFT response functions toward the change of the total number of electrons only. The chemical nature of the system and the specific interactions that are activated during the internal rotation indicate that changes in the external potential are not relevant for explaining such a low energy process.

Acknowledgment. This work was supported by FONDECYT through projects No. 1020534 and 7020534. A.T.L. is grateful to Université Joseph Fourier in Grenoble (France) for a Visiting Professor fellowship. We also thank CENG-CEA of Grenoble for grants of computer time. The authors thank Professor P. Fuentealba (Universidad de Chile) for helpful discussions.

References and Notes

(1) Steenken, S. *Chem. Rev.* **1989**, *89*, 503.
(2) Tuppurainen, K.; Lötjönen, S.; Laatikainen, R.; Vartiainen, T.; Maran, U.; Strandberg, M. *Mutat. Res.* **1991**, *247*, 97.
(3) Lenninger, Nelson, Cox, *Principles of Biochemistry*, 2nd edition; Worth Publishers Inc.: New York, 1993.
(4) Parr, R. G.; Yang, W. *Density Functional Theory of Atoms and Molecules*; Oxford University Press: New York, 1989.
(5) Sen, K. D., Ed.; *Structure and Bonding 80: Chemical Hardness*; Springer-Verlag: Berlin, 1993.
(6) Geerlings, P.; De Proft, F.; Langenaeker, W. *Density Functional Theory. A Bridge between Chemistry and Physics*; VUB University Press: Brussels, Belgium, 1998.
(7) Parr, R. G.; Donnelly, R. A.; Levy, M., Palke, W. E. *J. Chem. Phys.* **1978**, *68*, 3801.
(8) Pearson, R. G. *J. Am. Chem. Soc.* **1963**, *85*, 3533. Pearson, R. G. *Science* **1966**, *151*, 172.
(9) Parr, R. G.; Pearson, R. G. *J. Am. Chem. Soc.* **1983**, *105*, 7512.
(10) Pearson, R. G. *Inorg. Chem.* **1988**, *27*, 734.; Pearson, R. G. *J. Am. Chem. Soc.* **1988**, *110*, 7684.
(11) Pearson, R. G. *Coord. Chem. Rev.* **1990**, *100*, 403.
(12) Parr, R. G.; Yang, W. *J. Am. Chem. Soc.* **1984**, *106*, 4049.
(13) Yang, W.; Parr, R. G. *Proc. Natl. Acad. Sci. U.S.A.* **1985**, *82*, 6723.
(14) Hammond, G. S. *J. Am. Chem. Soc.* **1955**, *77*, 334.
(15) Leffler, J. E. *Science* **1953**, *117*, 340.
(16) See, for example: Pross, A. *Theoretical and Physical Principles of Organic Reactivity*; Wiley Interscience: New York, 1995.
(17) Marcus, R. A. *Annu. Rev. Phys. Chem.* **1964**, *15*, 155.
(18) Pearson, R. G. *J. Chem. Educ.* **1987**, *64*, 561. Parr, R. G.; Chattaraj, P. K. *J. Am. Chem. Soc.* **1991**, *113*, 1854. Chattaraj, P. K.; Liu, G. H.; Parr, R. G. *Chem. Phys. Lett.* **1995**, *237*, 171.
(19) Pearson, R. G. *Chemical Hardness: Applications from Molecules to Solids*; Wiley-VCH Verlag GMBH: Weinheim, Germany, 1997.
(20) Datta, D. *J. Phys. Chem.* **1992**, *96*, 2409.
(21) Chattaraj, P. K.; Nath, S.; Sannigrahi, A. B. *J. Phys. Chem.* **1994**, *98*, 9143.
(22) Chattaraj, P. K. *Proc. Indian Natl. Sci. Acad.- Part A* **1996**, *62*, 513.
(23) Chattaraj, P. K.; Sengupta, S. *J. Phys. Chem.* **1996**, *100*, 16126. Chattaraj, P. K.; Poddar, A. *J. Phys. Chem. A* **1998**, *102*, 9944. Chattaraj, P. K.; Poddar, A. *J. Phys. Chem. A* **1999**, *103*, 1274.
(24) Toro-Labbé, A. *J. Mol. Struct. (THEOCHEM)* **1988**, *180*, 209. Toro-Labbé, A. *J. Mol. Struct. (THEOCHEM)* **1990**, *207*, 247. Cárdenas-Jirón, G. I.; Toro-Labbé, A.; Bock, C. W.; Maruani, J. In *Structure and Dynamics of Non-Rigid Molecular Systems*; Smeyers, Y. G., Ed.; Kluwer Academic Publishers: New York, 1995; pp 97−120.
(25) Toro-Labbé, A. *J. Phys. Chem. A* **1999**, *103*, 4398.
(26) Parr, R. G.; von Szenpály, L.; Liu, S. *J. Am. Chem. Soc.* **1999**, *121*, 1922.
(27) Chattaraj, P. K.; Pérez, P.; Zevallos, J.; Toro-Labbé, A. *J. Phys. Chem. A* **2001**, *105*, 4272. Pérez, P.; Toro-Labbé, A.; Contreras, R. *J. Am. Chem. Soc.* **2001**, *123*, 5527. Chattaraj, P. K.; Pérez, P.; Zevallos, J.; Toro-Labbé, A. *J. Mol. Struct. (THEOCHEM)* **2002**, *580*, 171. Pérez, P.; Toro-Labbé, A.; Aizman, A.; Contreras, R. *J. Org, Chem.* **2002**, *67*, 4747. Jaque, P.; Toro-Labbé, A. *J. Chem. Phys.* **2002**, *117*, 3208.
(28) Maitland, G. C.; Rigby, M.; Smith, E. B.; Waheham, W. A. *Intermolecular Forces. Their Origin and Determination*; Oxford: New York, 1987. McQuarrie, D. A.; Simon, J. D. *Physical Chemistry. A Molecular Approach*; University Science Books: Sausalito, CA, 1997.
(29) Chattaraj, P. K.; Fuentealba, P.; Jaque, P.; Toro-Labbé, A. *J. Phys. Chem. A* **1999**, *103*, 9307. Hohm, U. *J. Phys. Chem. A* **2000**, *104*, 8418. Pérez, P.; Toro-Labbé, A. *Theor. Chem. Acc.* **2001**, *105*, 422. Jaque, P.; Toro-Labbé, A. *J. Phys. Chem. A* **2000**, *104*, 995. Pérez, P.; Toro-Labbé, A. *J. Phys. Chem. A* **2000**, *104*, 1557. Gutiérrez-Oliva, S.; Jaque, P.; Toro-Labbé, A. *J. Phys. Chem. A* **2000**, *104*, 8955.
(30) Politzer, P. *J. Chem. Phys.* **1987**, *86*, 1072. Fuentealba, P.; Reyes, O. *J. Mol. Struct. (THEOCHEM)* **1993**, *282*, 65. Ganthy, T. K.; Ghosh, S. K. J. *J. Phys. Chem.* **1993**, *97*, 4951. Simón-Manso, Y.; Fuentealba, P. *J. Phys. Chem. A* **1998**, *102*, 2029.
(31) Frisch, M. J.; Trucks, G. W.; Schlegel, H. B.; Scuseria, G. E.; Robb, M. A.; Cheeseman, J. R.; Zakrzewski, V. G.; Montgomery, J. A., Jr.; Stratmann, R. E.; Burant, J. C.; Dapprich, S.; Millam, J. M.; Daniels, A. D.; Kudin, K. N.; Strain, M. C.; Farkas, O.; Tomasi, J.; Barone, V.; Cossi, M.; Cammi, R.; Mennucci, B.; Pomelli, C.; Adamo, C.; Clifford, S.; Ochterski, J.; Petersson, G. A.; Ayala, P. Y.; Cui, Q.; Morokuma, K.; Malick, D. K.; Rabuck, A. D.; Raghavachari, K.; Foresman, J. B.; Cioslowski, J.; Ortiz, J. V.; Stefanov, B. B.; Liu, G.; Liashenko, A.; Piskorz, P.; Komaromi, I.; Gomperts, R.; Martin, R. L.; Fox, D. J.; Keith, T.; Al-Laham, M. A.; Peng, C. Y.; Nanayakkara, A.; Gonzalez, C.; Challacombe, M.; Gill, P. M. W.; Johnson, B. G.; Chen, W.; Wong, M. W.; Andres, J. L.; Head-Gordon, M.; Replogle, E. S.; Pople, J. A. *Gaussian 98*; Gaussian, Inc.: Pittsburgh, PA, 1998.
(32) Becke, A. D. *J. Chem. Phys.* **1993**, *98*, 5648.
(33) Lee, C.; Yang, W.; Parr, R. G. *Phys. Rev. B* **1988**, *37*, 785.
(34) Head-Gordon, M.; Pople, J. A.; Frisch, M. J. *Chem. Phys. Lett.* **1988**, *153*, 503. Frisch, M. J.; Head-Gordon, M.; Pople, J. A. *Chem. Phys. Lett.* **1990**, *166*, 275. Frisch, M. J.; Head-Gordon, M.; Pople, J. A. *Chem. Phys. Lett*. **1990**, *166*, 281.
(35) Orlov, V. M.; Smirnov, A. N.; Varshavsky, Ya. M. *Tetrahedron Lett.* **1976**, *48*, 4377. Hush, N. S.; Cheung, A. S. *Chem. Phys. Lett.* **1975**, *34*, 11.
(36) Hutter, M.; Clark, T. *J. Am. Chem. Soc.* **1996**, *118*, 7574.
(37) Politzer, P.; Abu-Awwad, F. *Theor. Chem. Acc*. **1998**, *99*, 83.
(38) Thewald, U.; Bugg, C. E.; Marsh, R. E. *Acta Crystallogr.* **1971**, *B27*, 2358. Destro, R.; Kistenmacher, T. J.; Marsh, R. E. *Acta Crystallogr.* **1974**, *B30*, 79. Held, D.; Pratt, D. W. *J. Am. Chem. Soc*. **1993**, *115*, 9708. Gorb, L.; Leszczynski, J. *J. Am. Chem. Soc*. **1998**, *120*, 5024.
(39) Chandra, A. K.; Uchimaru, T. *J. Phys. Chem. A* **2001**, *105*, 3578.
(40) Torrent-Sucarrat, M.; Luis, J. M.; Duran, M.; Solà, M. *J. Am. Chem. Soc.* **2001**, *103*, 7951.
(41) Tian, S. X.; Xu, K. Z. *Chem. Phys.* **2001**, *264*, 187. Bottcher, C. F. J. *Theory of Electric Polarization*; Elsevier: Amsterdam, 1993.
(42) Gutiérrez-Oliva, S.; Letelier, J. R.; Toro-Labbé, A. *Mol. Phys.* **1999**, *96*, 61. Gutiérrez-Oliva, S.; Jaque, P.; Toro-Labbé, A. In *Reviews in Modern Quantum Chemistry: A Celebration of the Contributions of Robert G. Parr*; Sen, K. D., Ed.; World Scientific Press: Singapore, 2002; p 966.
(43) Parr, R. G.; Bartolotti, L. J. *J. Am. Chem. Soc.* **1982**, *104*, 3801.